Synthesis, Structure and Physical Properties of the First One-Dimensional Phenalenyl-Based Neutral Radical Molecular Conductor

ARTICLE *in* JOURNAL OF THE AMERICAN CHEMICAL SOCIETY · MARCH 2004

Impact Factor: 12.11 · DOI: 10.1021/ja037864f · Source: PubMed

J|A|C|S
ARTICLES
Published on Web 01/20/2004

Synthesis, Structure and Physical Properties of the First One-Dimensional Phenalenyl-Based Neutral Radical Molecular Conductor

S. K. Pal,[†] M. E. Itkis,[†] R. W. Reed,[‡] R. T. Oakley,[‡] A. W. Cordes,[§] F. S. Tham,[†] T. Siegrist,[||] and R. C. Haddon*,[†]

Contribution from the Departments of Chemistry and Chemical & Environmental Engineering, University of California, Riverside, California 92521-0403, Department of Chemistry, University of Waterloo, Waterloo, Ontario N2L 3G1, Canada, Department of Chemistry and Biochemistry, University of Arkansas, Fayetteville, Arkansas 72701, and Bell Laboratories, Lucent Technologies, Murray Hill, New Jersey 07974

Received August 11, 2003; E-mail: haddon@ucr.edu

Abstract: We report the preparation, crystallization, and solid-state characterization of a benzyl-substituted spirobiphenalenyl radical. The crystal structure shows that the radical is monomeric in the solid state, with the molecules packed in an unusual one-dimensional (1-D) fashion that we refer to as a π-step stack. This particular mode of 1-D stacking is forced on the lattice arrangement by the presence of the orthogonal phenalenyl units that were specifically incorporated to prevent the crystallization of low-dimensional structures. The structure shows that this strategy is effective, and neighboring molecules in the stack can only interact via the overlap of one pair of active (spin-bearing) carbon atoms per phenalenyl unit, leading to the π-step structure in which the remaining four active carbon atoms per phenalenyl unit do not interact with nearest neighbor molecules. The magnetic susceptibility data in the temperature range 4−360 K may be fit to an antiferromagnetic Heisenberg $S = 1/2$ linear chain model with intrachain spin coupling $J = -52.3$ cm^{-1}. Despite the uniform stacking, the material has a room temperature conductivity of 1.4×10^{-3} S/cm and is best described as a Mott insulator.

Introduction

Although most organic compounds are insulators, McCoy[1] predicted over 80 years ago that some organic solids might exhibit high electrical conductivity, comparable with that of metals. A major breakthrough came with the discovery of charge-transfer (CT) salts based on 7,7,8,8-tetracyano-*p*-quinodimethane (TCNQ)[2] in 1960, after which many TCNQ-based CT salts with various donors were prepared and studied.[3] A new class of electron-transfer superconductors, based on the alkali metal fullerides A_3C_{60} (A = K, Rb, Cs) was discovered in 1991.[4,5] The fullerene-based superconductors are anion radical salts, different from tetramethyltetraselenafulvalene (TMTSF)[6] and ethylenedithiotetrathiafulvalene (ET) based[7] cation radical superconductors. Another important difference is the type of molecular structure and the dimensionality of the crystals. Fullerene-based superconductor crystals are three-dimensional, in contrast to the quasi-one- and two-dimensional electronic structures of $(TMTSF)_2X$ and $(ET)_2X$, respectively. In conventional inorganic conductors, such as Cu or Na, the atoms form close-packed structures in the solid state. They can be viewed as crystallized atomic free radicals. The atomic orbitals interact strongly with each other to form broad electronic energy bands of width $W > 3$ eV.[8] The HOMOs of these atoms (originating from s orbitals) are singly occupied and form half-filled (conduction) bands. These materials are good conductors as the electrons in the conduction bands can move freely in the lattice. In organic solids, such as the CT salts, the interactions between the molecules are weak, forming narrow bands ($W = \sim 0.5$ eV) in comparison with the inorganic metals.[9]

For some time we have attempted to prepare an intrinsic molecular metal, that is, a solid composed of a single molecular species that would function as a classical (mono)atomic metal

[†] University of California.
[‡] University of Waterloo.
[§] University of Arkansas.
[||] Lucent Technologies.

(1) McCoy, H. N.; Moore, W. C. Organic Amalgams: Substances With Metallic Properties Compound in Part of Non-Metallic Elements. *J. Am. Chem. Soc.* **1911**, *33*, 273−292.
(2) Kepler, R. G.; Bierstedt, P. E.; Merrifield, R. E. Electronic Conduction and Exchange Interaction in a New Class of Conductive Organic Solids. *Phys. Rev. Lett.* **1960**, *5*, 503−504.
(3) Siemons, W. J.; Bierstedt, P. E.; Kepler, R. G. Electronic Properties of a New Class of Highly Conductive Organic Solids. *J. Chem. Phys.* **1963**, *39*, 3523−3528.
(4) Haddon, R. C.; Hebard, A. F.; Rosseinsky, M. J.; Murphy, D. W.; Duclos, S. J.; Lyons, K. B.; Miller, B.; Rosamilia, J. M.; Fleming, R. M.; Kortan, A. R.; Glarum, S. H.; Makhija, A. V.; Muller, A. J.; Eick, R. H.; Zahurak, S. M.; Tycko, R.; Dabbagh, G.; Thiel, F. A. Conducting Films of C60 and C70 by Alkali Metal Doping. *Nature* **1991**, *350*, 320−322.
(5) Hebard, A. F.; Rosseinsky, M. J.; Haddon, R. C.; Murphy, D. W.; Glarum, S. H.; Palstra, T. T. M.; Ramirez, A. P.; Kortan, A. R., Superconductivity at 18K in Potassium-Doped C60. *Nature* **1991**, *350*, 600.
(6) Bechgaard, K.; Cowan, D. O.; Bloch, A. N. Synthesis of Organic Conductor TMTSF-TCNQ. *J. Chem. Soc., Chem. Commun.* **1974**, 937−938.
(7) Parkin, S. S. P.; Engler, E. M.; Schumaker, R. R.; Lagier, R.; Lee, V. Y.; Scott., J. C.; Greene, R. L. Superconductivity in a New Family of Organic Conductors. *Phys. Rev. Lett.* **1983**, *50*, 270−273.
(8) Thrower, P. A. *Materials in Today's World*; McGraw-Hill's Primis Custom: New York, 1996.

10.1021/ja037864f CCC: $27.50

Scheme 1

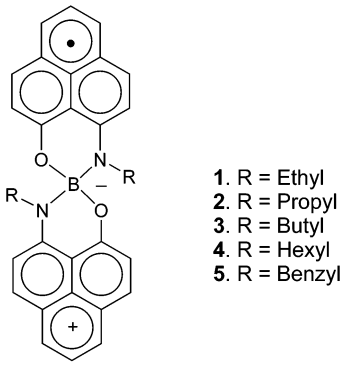

and superconductor.[10,11] This necessarily requires the crystallization of a neutral radical, and we have argued in favor of the phenalenyl system.[12−14] We have recently reported the first phenalenyl-based neutral radical conductor (**4**)[15] and, more recently, a class of dimeric phenalenyl-based neutral radical molecular conductors (**1**, **3**)[16,17] and their bistability in three physical channels.[18] (See Scheme 1.) A distinctive feature of these molecular solids is the absence of any obvious conducting pathway(s), and a very curious increase in conductivity at the phase transition.[17−19] These radicals do not stack in the solid state, and the intermolecular carbon···carbon contacts are all larger than the sum of the van der Waals distances. Compound **4** behaves as a free radical with one spin per molecule, indicating little interaction between the molecules in the solid state. Despite this, the radical shows the highest conductivity ($\sigma_{RT} = 0.05$ S/cm) of any neutral organic solid, and the conduction mechanism is presently not understood.

We have now crystallized compound **5**, another radical in the family of spirobis(1,9-disubstituted phenalenyl)boron compounds, which differs only in the alkyl substituent from previous members in the series (**1**, **2**, **3**, **4**), but adopts an entirely different solid-state structure. Although the idea of developing organic conductors based on neutral π-radicals has a number of merits, there are difficulties that must be surmounted. Apart from the problem of σ-dimerization, it is necessary to inhibit one-dimensional packing that is characteristic of many organic charge-transfer salts and to reduce the large on-site Coulombic correlation energy which leads to an insulating ground state in most of the half-filled band structures. In fact, the spiro(1,9-disubstituted phenalenyl)boron compounds were chosen with these considerations in mind. With respect to one-dimensional stacking this strategy has been effective, but in compound **5** a particularly unusual structure is observed, which is referred to as π-stepped. Below, we show that the conductivity of radical **5** is comparable with that of the previously reported radicals (**1**, **3**, **4**) and greater than that of the propyl radical (**2**).

Scheme 2

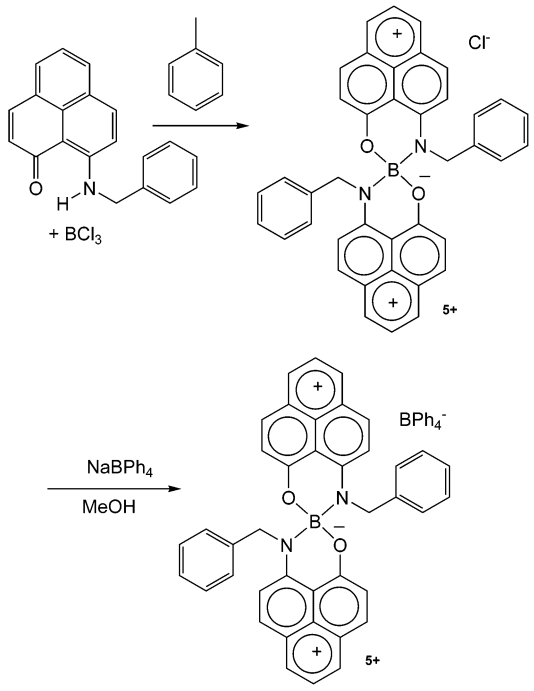

In the present paper, we report the synthesis, crystallization, and solid-state properties of radical **5**. We assess the strength of the interaction between the molecules in the lattice by using extended Hückel theory (EHT).

In the solid state, benzyl radical (**5**) does not form a simple σ- or π-dimer, nor does it remain strictly monomeric. In the case of benzyl radical (**5**), the unit cell contains four molecules, whereas the other radicals contain four (two π-dimers, **1** and **3**) or eight (**4**) monomers in the unit cell. In **5**, the phenalenyl units in the *x*- and *z*-directions pack perpendicular to each other, whereas the phenalenyl units in the *y*-direction are parallel to each other and packed in the π-step fashion. As shown by the band structure calculations, this provides a very effective conducting pathway in crystals of benzyl radical (**5**) even though only one of the active carbon atoms is involved in overlap with its nearest neighbor.

Results and Discussion

Preparation and Solution Properties of Radical 5. The synthesis of radical **5** followed the same basic procedure that was used to prepare radicals **1**, **3**, and **4**.[15,16] We prepared the benzyl variant via the chloride salt ($\mathbf{5}^+Cl^-$) but finally employed the tetraphenylborate anion to obtain the required solubility properties of the salt. Compound $\mathbf{5}^+BPh_4^-$ (Scheme 2) gave air-stable, but light-sensitive orange crystals that could be

(9) Haddon, R. C.; Ramirez, A. P.; Glarum, S. H. Electron-Electron Interactions in Organic Superconductors. *Adv. Mater.* **1994**, *6*, 316−322.
(10) Haddon, R. C. Design of Organic Metals and Superconductors. *Nature* **1975**, *256*, 394−396.
(11) Haddon, R. C. Quantum Chemical Studies in the Design of Organic Metals. III. Odd-Alternant Hydrocarbons (OAHs): The Phenalenyl (PLY) System. *Aust. J. Chem.* **1975**, *28*, 2343−2351.
(12) Haddon, R. C.; Wudl, F.; Kaplan, M. L.; Marshall, J. H.; Cais, R. E.; Bramwell, F. B. 1,9-Dithiophenalenyl System. *J. Am. Chem. Soc.* **1978**, *100*, 7629−7633.
(13) Haddon, R. C.; Chichester, S. V.; Stein, S. M.; Marshall, J. H.; Mujsce, A. M. Perchloro-7H-cycloprop[a]acenaphthylene and the Perchlorophenalenyl System. *J. Org. Chem.* **1987**, *52*, 711−712.
(14) Koutentis, P. A.; Chen, Y.; Cao, Y.; Best, T. P.; Itkis, M. E.; Beer, L.; Oakley, R. T.; Brock, C. P.; Haddon, R. C. Perchlorophenalenyl Radical. *J. Am. Chem. Soc.* **2001**, *123*, 3864−3871.
(15) Chi, X.; Itkis, M. E.; Patrick, B. O.; Barclay, T. M.; Reed, R. W.; Oakley, R. T.; Cordes, A. W.; Haddon, R. C. The First Phenalenyl-Based Neutral Radical Molecular Conductor. *J. Am. Chem. Soc.* **1999**, *121*, 10395−10402.
(16) Chi, X.; Itkis, M. E.; Reed, R. W.; Oakley, R. T.; Cordes, A. W.; Haddon, R. C. Conducting Pathways in Organic Solids: A Phenalenyl-Based Neutral Radical of Low Conductivity. *J. Phys. Chem. B* **2002**, *106*, 8278−8287.
(17) Chi, X.; Itkis, M. E.; Kirschbaum, K.; Pinkerton, A. A.; Oakley, R. T.; Cordes, A. W.; Haddon, R. C. Dimeric Phenalenyl-Based Neutral Radical Molecular Conductors. *J. Am. Chem. Soc.* **2001**, *123*, 4041−4048.
(18) Itkis, M. E.; Chi, X.; Cordes, A. W.; Haddon, R. C. Magneto-Opto-Electronic Bistability in a Phenalenyl-Based Neutral Radical. *Science* **2002**, *296*, 1443−1445.
(19) Huang, J.; Kertesz, M. Spin Crossover of Spiro-Biphenalenyl Neutral Radical Molecular Conductors. *J. Am. Chem. Soc.* **2003**, *125*, 13334−13335.

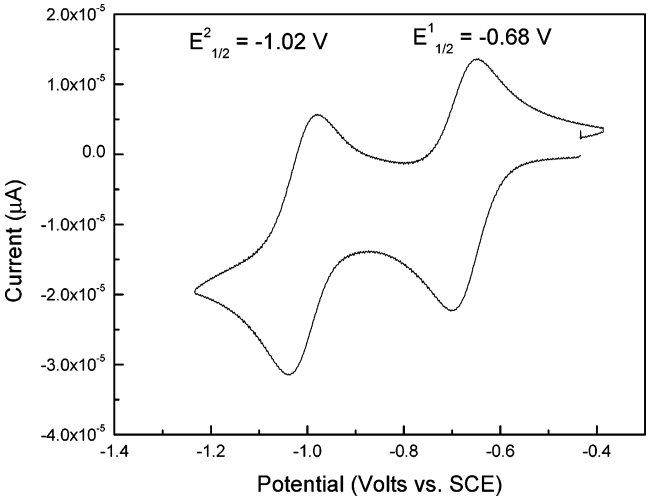

Figure 1. Cyclic voltammetry of $\mathbf{5}^{+}BPh_4^{-}$ in acetonitrile, reference to SCE via internal ferrocene (not shown).

Scheme 3

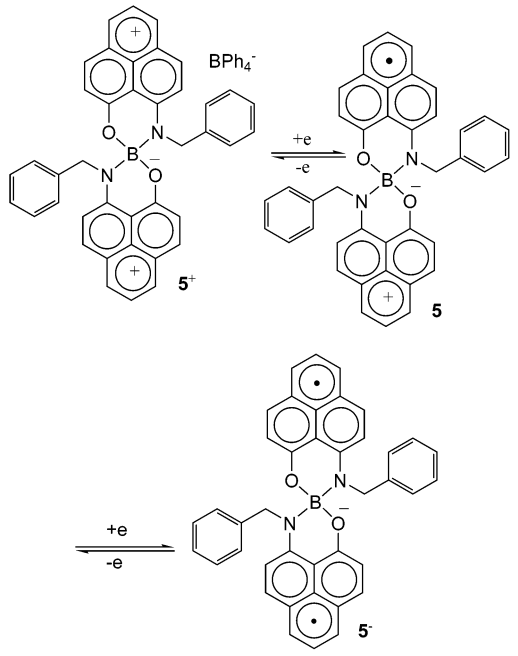

purified by recrystallization from methanol and dichloromethane to give material suitable for radical preparation and crystal growth.

The electrochemistry of $\mathbf{5}^{+}BPh_4^{-}$ is presented in Figure 1, where it may be seen that the compound shows a well-behaved double reduction. The first reduction potential corresponds to reduction of the cation to radical, and the second reduction potential corresponds to radical to anion reduction. The disproportionation potential $\Delta E^{2-1} = (E^{2}_{1/2} - E^{1}_{1/2}) = -0.33$ V, is very similar to the values found for the alkyl-substituted compounds (**1**−**4**). The ΔE^{2-1} value largely determines the on-site Columbic correlation energy (U) in the solid state, and is well established as an important discriminator for organic metals.[20,21]

(20) Garito, A. F.; Heeger, A. J. The Design and Synthesis of Organic Metals. *Acc. Chem. Res.* **1974**, *7*, 232−240.
(21) Torrance, J. B. The Difference Between Metallic and Insulating Salts of Tetracyanoquinodimethane (TCNQ): How to Design an Organic Metal. *Acc. Chem. Res.* **1979**, *12*, 79−86.

Table 1. Crystal Data for Benzyl Radical (**5**)

formula	$C_{40}H_{28}BN_2O_2$	
formula weight	579.45	
temperature	223(2) K	
crystal system	monoclinic	
space group	*C*2/*c*	
unit cell dimensions	$a = 23.386(2)$ Å	$\alpha = 90°$
	$b = 5.7326(6)$ Å	$\beta = 97.782(2)°$
	$c = 20.963(2)$ Å	$\gamma = 90°$
volume	2784.6(5) Å^3	
Z	4	
crystal size	$0.55 \times 0.19 \times 0.17$ mm^3	
goodness of fit on F^2	1.038	
final R indices [$I > 2\sigma(I)$]	$R_1 = 0.0396$, $wR_2 = 0.1027$	
R indices (all data)	$R_1 = 0.0524$, $wR_2 = 0.1142$	

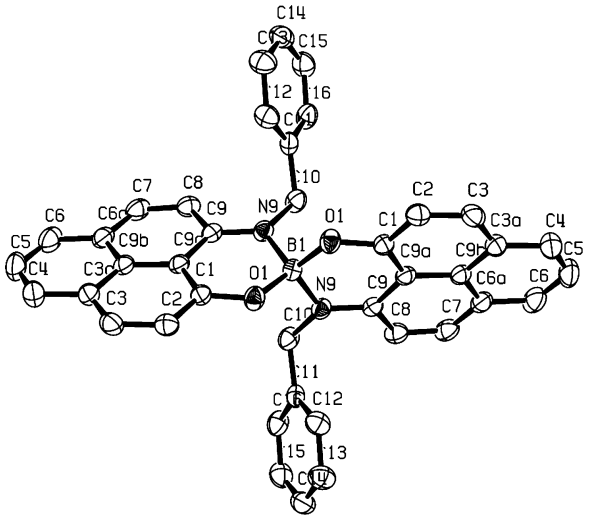

Figure 2. ORTEP diagram of **5**.

We crystallized **5** by using a chemical reductant in an H-cell and obtained an excellent yield of high-quality, long black needles of the radical. Cobaltocene was used as reductant because the oxidation potential of cobaltocene ($E^{1/2} = -0.91$ V)[22] falls between the two reduction potentials of $\mathbf{5}^{+}BPh_4^{-}$. To prepare high-quality crystals, the H-cell was loaded in a drybox and the solvent (acetonitrile) was degassed three times on a vacuum line before mixing the reductant and salt. Crystal growth started on the glass frit after 3 days, and the crystals reached their optimum size and quality in about 7−10 days. Although solutions of the radical are extremely oxygen sensitive, the crystals were stable enough to allow us to obtained chemical analyses, X-ray crystal structure, and other solid-state measurements after handling the crystal in the air.

X-ray Crystal Structure of 5. The structure was determined at $T = 223$ K, and there are four molecules of **5** in the unit cell. Crystals of **5** belong to the monoclinic space group *C*2/*c*. Table 1 provides crystal data, and Figure 2 shows an ORTEP drawing of the molecule together with the atom numbering. The most important point for our purposes is the absence of simple σ- or π-dimerization, even though we did not employ bulky substituents at the active position of the phenalenyl nucleus in order to suppress intermolecular carbon···carbon bond formation.[12,13] The unit cell of crystalline **5** is shown in Figure 3.

(22) Robbins, J. L.; Edelstein, N.; Spencer, B.; Smart, J. C. Syntheses and Electronic Structure of Decamethylmetallocenes. *J. Am. Chem. Soc.* **1982**, *104*, 1882−1893.

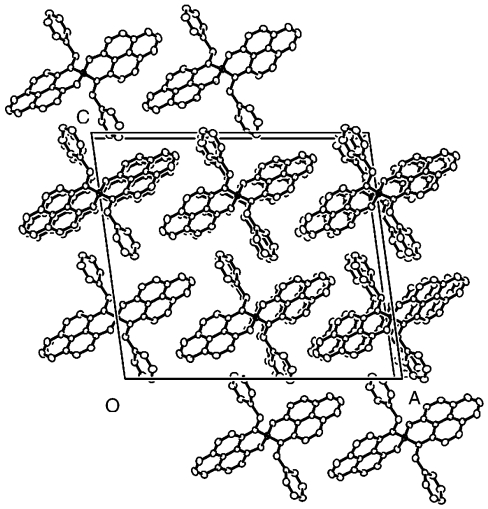

Figure 3. Unit cell of crystalline **5**; viewed down the *y*-axis.

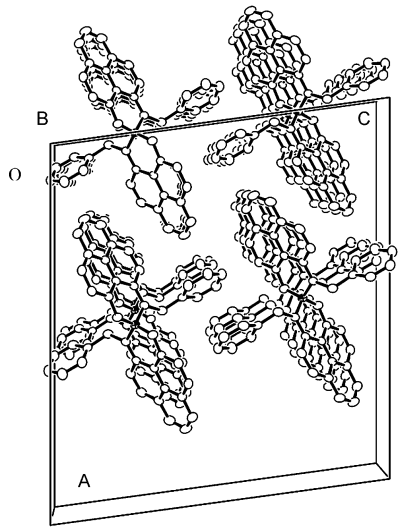

Figure 4. Packing along the *y*-direction.

In the *x*-and *z*-directions the phenalenyl rings are almost perpendicular to one another (the interplanar angle is around 80°). The closest C···C distance between phenalenyl units varies from 3.54 to 3.66 Å, whereas the closest distance for the benzyl substituent is 3.76 Å. There are no interradical distances that are shorter than van der Waals contacts in these directions. The packing in the *y*-direction is quite different from the packing in the *x*- and *z*-directions and also contrasts with that seen in the other boron radicals (**1**−**4**). The molecules form a one-dimensional stack along the *y*-axis (Figure 4), but offset with respect to nearest neighbors. The stacking (*y*) axis corresponds to the needle axis of the crystal. The phenyl and the phenalenyl rings on both sides of the boron are packed in a π-step as shown in Figure 4 and 5. On the basis of the one-dimensional structure along *y*, we looked for a superstructure, but we did not find any reflections characteristic of a superlattice. The closest carbon···carbon distances between molecules along the *y*-direction are 3.47 and 3.58 Å (Figure 5). The molecules are almost superimposed at these positions, so the overlap between molecules is effective (see band structure discussion below), despite the comparatively large separation, which is greater than the sum of the van der Waals separations for carbon atoms.

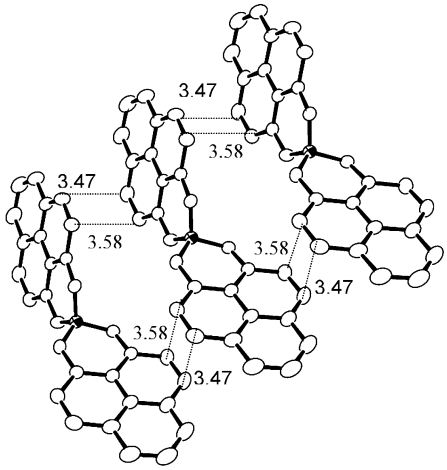

Figure 5. One-dimensional π-step structure along the *y*-axis.

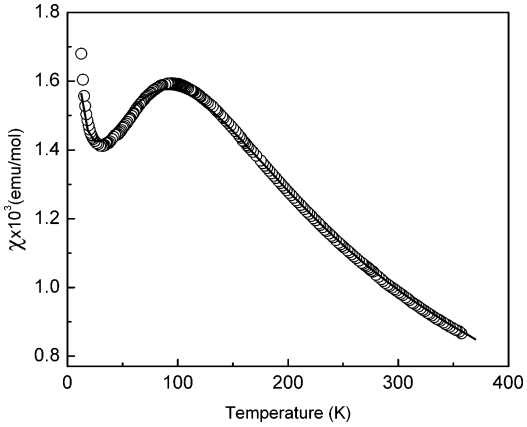

Figure 6. Magnetic susceptibility of **5** as a function of temperature. The measured results are shown as open circles, while the solid line represents the best fit to the 1-D $S = 1/2$ antiferromagnetic Heisenberg model (see text) with $J = -52.3$ cm^{-1}, $g = 2.029$, and impurity spin concentration $P = 0.38\%$.

These interatomic distances may be compared with the mean plane separations seen in the ethyl radical (**1**): 3.18 Å ($T =$ 100 K, diamagnetic) and 3.31 Å ($T = 173$ K, paramagnetic). In the π-dimer radicals **1** and **3** there is almost complete superposition of all six active carbon atoms of the phenalenyl nucleus, and this apparently accounts for the differences between the magnetism (see below) of the two classes of radicals.

Magnetic Susceptibility of 5. The temperature dependence of the magnetic susceptibility (χ) of **5** is presented in Figure 6. At high temperatures ($T > 200$ K), the magnetic data can be described by the Curie−Weiss law $\chi = C/(T - \theta)$ with Weiss constant $\theta = -115$ K and Curie constant $C = 0.410$ (emu·K)/mol. This is 9% higher than the expected value of C (0.376 (emu·K)/mol) for a neutral radical crystal with one unpaired spin per molecule and a *g*-value of 2.0026. The negative Weiss constant corresponds to an antiferromagnetic interaction between the unpaired spins. Strong deviation from the Curie−Weiss model is observed below 150 K with a broad maximum in the magnetic susceptibility around $T_{max} = 94$ K. In compounds **1** and **3** the deviation from Curie behavior was a result of a structural phase transition (dimerization) with singlet state coupling of the spins.[16,18] The low-temperature X-ray data of **5** show no sign of such structural changes or superstructure. On the other hand, the crystal structure and band structure calculations (see below) show that **5** crystallizes as a one-dimensional

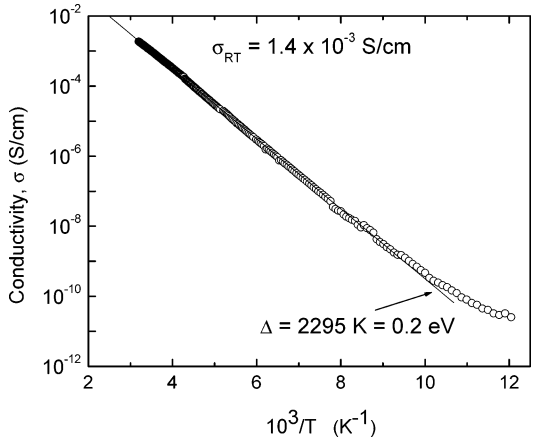

Figure 7. Single-crystal conductivity of **5** as a function of temperature, measured along the needle axis (*b*).

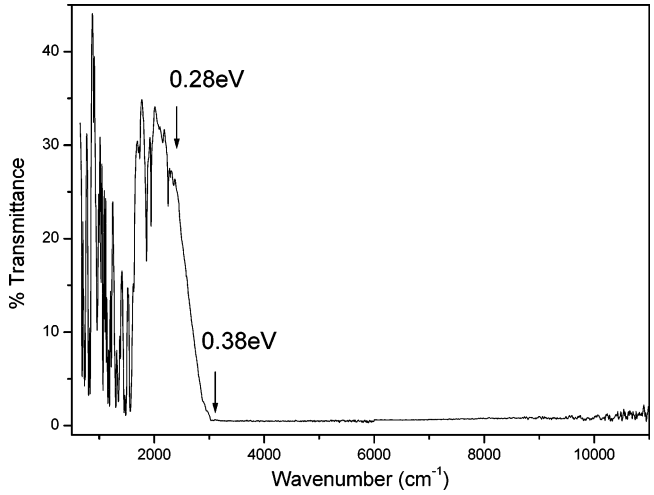

Figure 8. Single-crystal IR and UV−visible transmission spectrum of crystalline **5**.

chain. Thus, we used the Bonner−Fisher model for the $S = 1/2$ antiferromagnetic Heisenberg chain of isotropically interacting spins[23] to fit $\chi(T)$ for **5**. In addition to the Bonner−Fisher term χ_{BF},[23] an impurity term PC_{IM}/T was added to account for the low-temperature ($T < 20$ K) paramagnetic tail, so that $\chi(T) = (1 - P)\chi_{BF} + P(C_{IM}/T)$, where P is the fractional concentration of impurity spins and χ_{BF} is the usual analytic function with intrachain exchange constant (J) and g-value, as parameters;[24] C_{IM} is the Curie constant for the paramagnetic contribution of the impurities. The best fit parameters are $J = -52.3$ cm^{-1}, $g = 2.029$, and $P = 0.38\%$. The position of the maximum in $\chi(T)$ gives a similar value of $|J| = kT_{MAX}/1.282 = 50.95$ cm^{-1}.[23] The fit obtained over the temperature range 15−360 K (Figure 6) confirms the applicability of the one-dimensional $S = 1/2$ Heisenberg model[23] to compound **5**.

Electrical Resistivity of 5. The electrical conductivity (σ) of crystalline **5** was measured using four-probe contacts along the needle axis (*b*-axis of the unit cell) using a conductive paste. A number of crystals were evaluated over the temperature range from 80 to 330 K with identical results. Below 80 K the resistance of the crystals of **5** exceeds 10^{12} ohm, which is the limit of our experimental setup. The room-temperature conductivity of **5** is comparable with that of radical **1** (1.0×10^{-2} S/cm), **3** (2.4×10^{-2} S/cm), and **4** (4.9×10^{-2} S/cm)[16−18] and is 3 orders of magnitude higher than that of **2** (1.4×10^{-6} S/cm).[16] The conductivity shows a semiconducting temperature dependence with activation energy $\Delta = 0.2$ eV (Figure 7), which is discussed in later sections.

Electronic Excitations in Solid State 5. To obtain further information on the electronic structure, we measured the absorption spectrum of crystalline **5**. This is possible because of the needlelike morphology of the crystals, some of which are quite thin and are suitable for transmission spectroscopy.

The results are presented in Figure 8, where we show transmittance (T) measurements made on a single crystal. As may be seen, we find an optical energy gap E_g(optical) ≈ 0.38 eV ($\sim$3000 cm^{-1}) and the spectrum remains opaque past 10 000 cm^{-1} due to very strong bandlike excitations that extend throughout this region of the spectrum. This latter finding is unusual, as the absorptions in the other radicals such as **4** do not extend past 8000 cm^{-1}.[15] The absorption in the mid-IR, between 400 and 2900 cm^{-1}, is due to the molecular vibrations of the radical **5**. Note that the optical gap (E_g, Figure 8) is commensurate with the conductivity gap (Δ, Figure 7), as $E_g \approx 2\Delta$ is expected for an intrinsic semiconductor, and this suggests that these energy gaps have a common origin.

Band Electronic Structure of 5. We carried out extended Hückel theory (EHT) band structure calculations[25] on the crystal structure. Such calculations have been very useful in understanding the electronic structure of organic molecular superconductors[9] and thin-film field effect transistors[26] but cannot be expected to provide a complete picture of the electronic structure in situations where the tight-binding approximation is not applicable.

Figure 9 shows the results obtained for band structure calculations carried out on the lattice found in the X-ray crystal structure. The eight bands shown in Figure 9 are derived from the two LUMOs of $\mathbf{5}^+$, for each of the four molecules of **5** in the unit cell; basically these consist of the symmetric and antisymmetric combinations of the 1,9-disubstituted phenalenyl LUMO.[15,27] Alternatively they can be viewed as arising from the nonbonding molecular orbitals[10,11] of each of the eight phenalenyl units in the unit cell. In this picture these eight orbitals now accommodate a total of four electrons, leading to a quarter-filled band complex with two filled and six vacant bands. The tight binding picture fails, of course, because the magnetic susceptibility shows that the electrons are unpaired in this compound over the temperature range $T > 100$ K. Furthermore the band calculations suggest that the energy bands along b^* cross the Fermi level, and thus predict metallic behavior.

It may be seen that the band dispersion found along the π-step direction in **5** is much higher than in the other boron radicals (**1**, **3**, and **4**). The maximum dispersions are 0.045 eV (along a^*), 0.369 eV (b^*), and 0.052 eV (c^*) in **5**; the corresponding

(23) Bonner, J. C.; Fisher, M. E. Linear Magnetic Chains with Anisotropic Coupling. *Phys. Rev.* **1964**, *135*, A640.
(24) Estes, W. E.; Gavel, D. P.; Hatfield, W. E.; Hodgson, D. J. Magnetic and Structural Characterization of Dibromo- and Dichlorobis(thiazole)copper-(II). *Inorg. Chem.* **1978**, *17*, 1415−1421.
(25) Hofmann, R. *Solids and Surfaces*; VCH: New York, 1988.
(26) Haddon, R. C.; Siegrist, T.; Fleming, R. M.; Bridenbaugh, P. M.; Laudise, R. A. Band Structures of Organic Thin-Film Transistor Materials. *J. Mater. Chem* **1995**, *5*, 1719−1724.
(27) Haddon, R. C.; Chichester, S. V.; Marshall, J. H. Electron Delocalization in 9-Oxidophenalenone Complexes of Boron and Beryllium. *Tetrahedron* **1986**, *42*, 6293−6300.

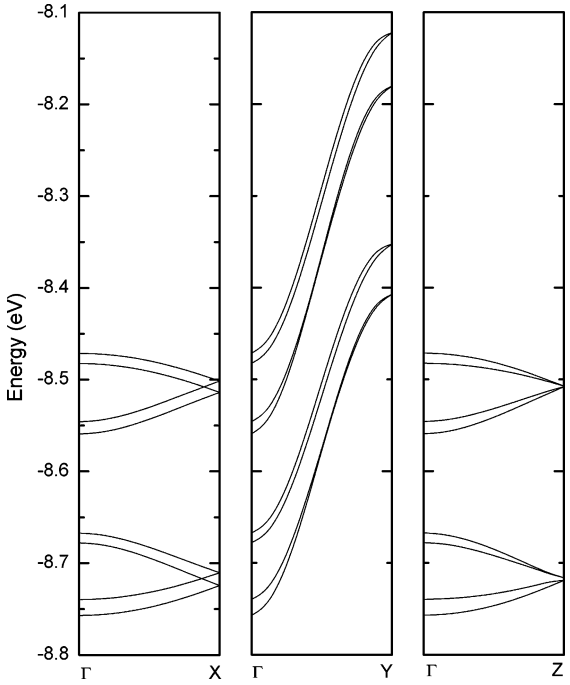

Figure 9. EHT band structure calculated for the experimental structure of crystalline **5**.

values in **4** are 0.036 eV (*a**), 0.075 eV (*b**), and 0.025 (*c**). Thus, it seems that there is a clear structural difference between **1**−**4** and the newly isolated **5** that is captured, at least to some extent, by the EHT band structure calculations.

The band calculations for crystalline **5** suggest substantial dispersion along *b**, and that all of the bands in this direction in reciprocal space cross the Fermi level; this statement holds whether the four electrons in the Brillouin zone populate the orbitals in pairs or singly (as suggested over most of the temperature range by the magnetic measurements). This is the first of the phenalenyl-based neutral radical conductors to possess a 1-D electronic structure and the first to possess significant band dispersion in the solid state (greater than 0.1 eV). Although the calculations fail to properly describe the electronic structure of **5**, the high band dispersion is reflected in the electronic spectrum (Figure 9), where the width of the bandlike absorptions is far greater than has been found for the other members of this series (**1**−**4**).[15]

The properties of the previously isolated phenalenyl-based neutral radical conductors remain largely unexplained,[15−17] and the same now holds for the 1-D π-step compound **5**. In contradiction to the structural and band structure data, the compound is clearly not metallic, but we have been unable to find a superlattice. Based on the magnetic susceptibility data for **5**, two-electron localization schemes (such as Figure 10c), seem unlikely due to the fact that the fraction of Curie spins does not fall below 50% and thus there is never full spin pairing. Thus the one-electron EHT band structure calculations fail to explain the Curie-type behavior of the magnetic susceptibility at high temperatures (Figure 6) and the nonmetallic temperature dependence of the conductivity (Figure 7).

The combination of electrical and magnetic properties observed for **5** is typical of a Mott insulator,[28−30] in which the unpaired spins are localized due to the predominance of the

(28) Mott, N. F. *Metal-Insulator Transitions*; Taylor & Francis: 1990.

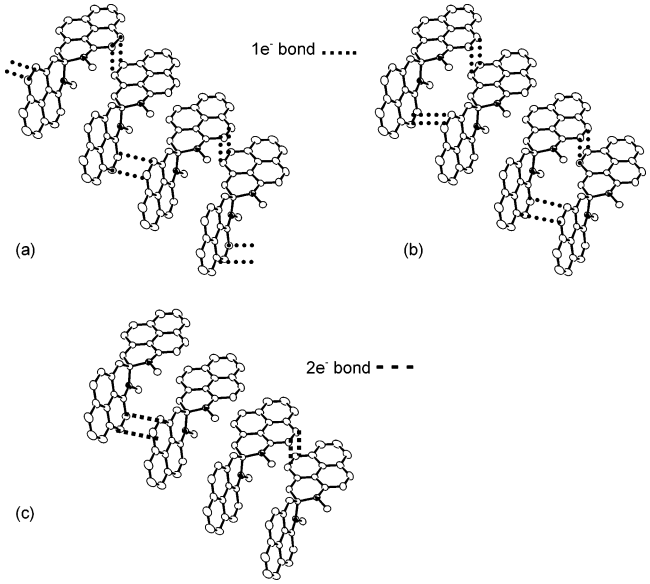

Figure 10. Possible localization schemes for crystalline **5**.

Coulomb interaction U over the transfer integral t. Thus the magnetic data are well described in terms of a one-dimensional $S = 1/2$ antiferromagnetic Heisenberg chain with $J = -52.3$ cm^{-1} (Figure 6).[23,24] The nonmetallic character of the conductivity (Figure 7) would then be the result of the localization of unpaired electrons due to their Coulombic repulsion or the large intermolecular separation.[28−30] In this picture the energy gaps that are apparent in the conductivity (2Δ, Figure 7), and the excitation spectrum (E_g, Figure 8), arise from the on-site Coulomb correlation energy. However, these values are comparable to the band dispersion along the *b*-axis that is calculated from the EHT calculations ($W \sim 0.4$ eV), and in the final analysis we cannot provide a self-consistent account of the electronic structure of the compound.

Conclusion

The properties of spirobiphenalenyls continue to challenge our understanding of conducting organic molecular crystals, and further work will be necessary to rationalize their behavior. Each new compound provides its own challenges, and even for the familiar 1-D stacking pattern that occurs in **5**, we find little analogy with the organic charge-transfer salts. In crystalline **5**, it is possible that the unusual behavior is related to what we have termed the π-step structure. Adoption of the π-step structure seems to be a response to the perpendicular π-systems that are present in **5**, which preclude the formation of a simple 1-D stacked structure in which a large fraction of the spin-bearing atoms undergo effective overlap with nearest neighbors in the stack. The structural data and band structure calculations suggest a metallic ground state for **5**, but at all temperatures we find semiconducting behavior of the conductivity and magnetism. The magnetic properties can be fit to the 1-D Bonner−Fisher model of localized antiferromagnetic spins in a Mott insulator regime.

(29) Yoneyama, N.; Miyazaki, A.; Enoki, T.; Saito, G. Magnetic Properties of TTF-Type Charge Transfer Salts in Mott Insulator Regime. *Bull. Chem. Soc. Jpn.* **1999**, *72*, 639−651.
(30) Whangbo, M. H. Mott-Hubbard condition for electronic localization in the Hartee-Fock band theory. *J. Chem. Phys.* **1979**, *70*, 4963−4966.

Experimental Section

Materials. Boron trichloride (Aldrich), sodium tetraphenylborate (Aldrich), and cobaltocene (Strem) were all commercial products and were used as received. 9-Hydroxy-1-oxophenalene was synthesized according to literature procedures.[31] Toluene was distilled from sodium benzophenone ketyl immediately before use. Acetonitrile was distilled from P_2O_5 and then redistilled from CaH_2 immediately before use.

9-*N*-Benzyl-1-oxophenalene. A mixture of 9-hydroxy-1-oxophenalene (0.98 g, 0.005 mol) and benzylamine (10 mL) were refluxed for 10 h in argon. After cooling, yellow crystals were formed and separated by filtration. The crude product was purified by column chromatography on Al_2O_3 with $CHCl_3$ to give a yellow solid (1.3 g, 92%). Further purification was done by crystallization from hexane. mp 128 °C. ^{1}H NMR ($CDCl_3$): δ 12.58 (b, 1H), 7.94 (d, 1H), 7.85−7.89 (m, 3H), 7.29−7.46 (m, 6H), 7.17 (d, 1H), 7.01 (d, 1H), 4.81 (d, 2H). Calcd for $C_{20}H_{15}NO$: C, 84.19; H, 5.30; N, 4.91. Found: C, 84.06; H, 5.28; N, 5.03.

Preparation of 5^+Cl^-. 9-*N*-Benzyl-1-oxophenalene (1.6 g, 0.0056 mol) in toluene (50 mL) was treated with boron trichloride in dichloromethane (2.7 mL, 0.0027 mol) under argon in the dark, and the mixture was stirred for overnight at room temperature. The yellow solid was isolated by filtration (1.6 g, 96%). IR (ATR, 4000−600 cm^{-1}): 3062(w), 3041(w), 3029(w), 1628(s), 1582(s), 1508(w), 1382(w), 1314(w), 1296(s), 1243(m), 1188(w), 1159(w), 1050(w), 1012(w), 874-(w), 844(m), 816(w), 760(w), 739(m), 698(m).

Preparation of $5^+BPh_4^-$. A solution of 0.72 g of $NaBPh_4$ in 10 mL of MeOH was added to a solution of 5^+Cl^- (0.78 g) in 30 mL of MeOH. An orange precipitate formed immediately. The mixture was stirred for 15 min, and 0.19 g (15%) of orange solid was separated by filtration and stored in the dark. The crude product can be purified by recrystallization from dichloromethane/methanol mixture. ^{1}H NMR (CD_3CN): δ 8.51 (d, 2H), 8.29−8.39 (m, 6H), 7.84 (t, 2H), 7.22−7.30 (m, 22H), 6.99 (t, 8H), 6.84 (t, 4H), 4.79 (q, 4H). IR (4000−600 cm^{-1}): 3050(w), 3031(w), 2995(w), 2981(w), 1624(m), 1595(w), 1583-(w), 1569(s), 1508(m), 1502(m), 1460(w), 1380(w), 1350(w), 1292-(s), 1238(m), 1191(m), 1165(w), 1128(w), 1066(m), 1053(s), 993(m), 957(w), 882(s), 840(s), 748(m), 731(s), 706(s). Anal. Calcd for $C_{64}H_{48}B_2N_2O_2 \cdot CH_2Cl_2$: C, 79.37; H, 5.12; N, 2.84; B, 2.19. Found: C, 79.77; H, 5.00; N, 3.03; B, 2.39.

Crystallization of 5. An invertable H-cell with a glass D frit was loaded in a drybox. A solution of 110 mg of $5^+BPh_4^-$ in 15 mL of dry acetonitrile was placed in one container, and 26.5 mg of $CoCp_2$ dissolved in 15 mL of dry acetonitrile was placed in the other container. The containers were attached to the inverted H-cell in the drybox. The H-cell was removed from the drybox and attached to the vacuum line, and the containers were taken through three cycles of freeze, pump, and thaw to degas the solutions. The H-cell was inverted slowly, and the solutions were allowed to diffuse through the glass frit. After sitting in the dark for 1 week the cell yielded 25 mg of black shining needles. IR (ATR, 4000−600 cm^{-1}): 3056(w), 3029(w), 1628(w), 1578(m), 1570(m), 1535(w), 1472(w), 1427(m), 1311(m), 1287(m), 1246(m), 1208(m), 1188(m), 1143(s), 1118(m), 1060(m), 1013(s), 964(s), 930-(s), 891(m), 827(s), 804(s), 769(s), 738(s). Anal. Calcd for $C_{40}H_{28}BN_2O_2$: C, 82.91; H, 4.87; N, 4.83; B, 1.87. Found: C, 82.33; H, 4.78; N, 5.30; B, 1.87.

X-ray Crystallography. Data were collected on a Bruker SMART 1000 platform-CCD X-ray diffractometer system (Mo radiation, λ = 0.710 73 Å, 50 kV/40 mA power) at 223 K. The black crystal gave a monoclinic unit cell (space group $C2/c$, $z = 4$), with unit cell parameters a = 23.386(2) Å, b = 5.7326(6) Å, c = 20.963(2) Å, β = 97.782(2)°, and V = 2784.6(5) Å^3. The structure was refined with 8590 reflections, yielding R [$I > 2\sigma(I)$], $R_1 = 0.0396$, $wR_2 = 0.1027$, and R indices for all data $R_1 = 0.0524$ and $wR_2 = 0.1142$ (Table 1). Full details, including bond lengths and bond angles, are given in the Supporting Information.

Magnetic Susceptibility Measurements. The magnetic susceptibility of **5** was measured over the temperature range of 4−357 K on a George Associates Faraday balance operating at 0.5 T.

Electron Paramagnetic Resonance Measurements. The electron paramagnetic resonance spectrum of **5** was measured on a Bruker EMX EPR spectrometer. A single crystal of **5** was mounted in perpendicular and parallel geometries with respect to the magnetic field by use of a pedestal inserted into a 0.5 mm EPR tube.

Conductivity Measurements. The single-crystal conductivity, σ, of **5** was measured in a four-probe configuration. The in-line contacts were made with silver paint. The sample was placed on a sapphire substrate, and electrical connections between the silver paint contacts and substrate were made by thin, flexible 25 μm diameter silver wires to relieve mechanical stress during thermal cycling of the sample. The temperature dependence of the conductivity was measured in the range 330−80 K. The data are presented for a crystal with dimensions 2.00 × 0.65 × 0.12 mm^3.

The conductivity was measured in a custom-made helium variable-temperature probe using a Lake Shore 340 temperature controller. A Keithley 236 unit was used as a voltage source and current meter, and two 6517 Keithley electrometers were used to measure the voltage drop between the potential leads in a four-probe configuration.

Single-Crystal IR and UV−vis Transmission Spectroscopy. The infrared transmission measurements were carried out on an FTIR Nicolet Nexus 670 ESP spectrometer integrated with a Continuum Thermo-Nicolet FTIR microscope.

Band Structure Calculations. The band structure calculations made use of a modified version of the extended Hückel theory (EHT) band structure program supplied by M.-H. Whangbo. The parameter set is chosen to provide a reasonably consistent picture of bonding in heterocyclic organic compounds.[26,32]

Acknowledgment. This work was supported by the Office of Basic Energy Sciences, Department of Energy, under Grant DE-FG032-97ER45668 and by DOD/DARPA/DMEA under Award No. DMEA90-02-2-0216.

Supporting Information Available: Tables of crystallographic and structural refinement data, atomic coordinates, bond lengths and angles, and anisotropic thermal parameters (PDF). This information is available free of charge via the Internet at http://pubs.acs.org.

JA037864F

(31) Haddon, R. C.; Chichester, S. V.; Mayo, S. L. Direct Animation of 9-Hydroxyphenalenone to Produce 9-Aminophenalenone and Related Compounds. *Synthesis* **1985**, 639−641.

(32) Cordes, A. W.; Haddon, R. C.; Oakley, R. T.; Schneemeyer, L. F.; Waszczak, J. V.; Young, K. M.; Zimmerman, N. M. Molecular Semiconductors from Bifunctional Dithia- and Diselenadiazolyl Radicals. Preparation and Solid-State Structural and Electronic Properties of 1,4-[(E_2N_2C)C_6H_4-(CN_2E_2)] (E = S, Se). *J. Am. Chem. Soc.* **1991**, *113*, 582−588.